Journal of Chromatography, 630 (1993) 21-35
Elsevier Science Publishers B.V., Amsterdam

CHROM. 24 724

Modeling of the adsorption behavior and the chromatographic band profiles of enantiomers

Behavior of methyl mandelate on immobilized cellulose

Frederic Charton*, Stephen C. Jacobson and Georges Guiochon

Department of Chemistry, University of Tennessee, Knoxville, TN 37996-1501 (USA) and Division of Analytical Chemistry, Oak Ridge National Laboratory, Oak Ridge, TN 67831-6120 (USA)

(First received August 25th, 1992; revised manuscript received October 27th, 1992)

ABSTRACT

The adsorption isotherms of (−)- and (+)-methyl mandelate from a hexane-isopropanol (90:10) solution were measured on a chromatographic column packed with Cmethylcellulose tribenzoate coated on silica. These isotherms are accounted for by a bi-Langmuir isotherm model, the two Langmuir terms having widely different initial slopes and saturation capacities, but each term having the same saturation capacity for the two enantiomers. The competitive isotherms were also measured. They are in excellent agreement with the prediction of a competitive bi-Langmuir model based on the single-component isotherms. The individual band profiles are in agreement with the profiles calculated from these isotherms. Thus, a simplified competitive isotherm can be used to model a separation on a chiral stationary phase the recognition mechanism of which is not well identified and the adsorption behavior of which is certainly not ideal.

INTRODUCTION

It has been proved [1,2] that the enantiomers of pharmaceuticals often differ in their pharmacological and side-effects. They can even have opposite biological activities. Thus, drug manufacturers are now required to study the physiological properties of each enantiomer, and can be compelled to produce one of them pure [3]. Different methods are available for the separation of enantiomers [4]. In connection with the investigation of the differential pharmacological properties of enantiomeric drugs, the direct chromatographic resolution of racemic mixtures on chiral stationary phases (CSPs) has been extensively studied in the recent past, but essentially for analytical purposes [5].

For preparative purposes, stereoselective synthesis and purification by crystallization are the preferred approaches. If these methods cannot be implemented, industrial-scale preparative chromatography on CSPs becomes an attractive separation process for enantiomers. This process is expensive, however, and to reduce its contribution to the total production costs it must be optimized, which is difficult to do correctly with a purely empirical approach because of the number of parameters involved and the intricacy of their interactions. Although it has been suggested that displacement chromatography could hold some advantages over elution for the separation of enantiomers [6], the optimization of the experimental conditions is even more complex in displacement than in elution chromatography. Furthermore, the current trend in

Correspondence to: G. Guiochon, Department of Chemistry, University of Tennessee, Knoxville, TN 37996-1501, USA.

* On leave from the Laboratoire des Sciences du Genie Chimique, ENSIC, Nancy, France.

0021-9673/93/$06.00

preparative chromatography is towards the use of new operating schemes, such as simulated moving bed, as alternatives to the classical elution chromatography [7,8]. In this event an empirical optimization cannot succeed, and a more rigorous approach is necessary.

The fundamentals of the optimization of overloaded chromatography have been studied using the analytical solution of the ideal model [9,10] and numerical calculations based on the equilibrium-dispersive model [11]. Excellent agreement has been reported in several instances between experimental and calculated results regarding optimization [12, 13]. The main practical difficulty is in the modeling of the competitive equilibrium isotherms. More experimental data are needed in this area.

The modeling of enantioseparations on immobilized bovine serum albumin (BSA) [13–15] and on microcrystalline cellulose triacetate [16] has already been undertaken successfully. The choice of a suitable isotherm model depends considerably, however, on the retention mechanism. There are numerous CSPs, which differ in the nature of their chiral discriminator, and hence in their chiral recognition mechanism. A number of them must be investigated in order to compare their properties and to attempt the derivation of general rules. The main object of this work is the study of enantiomeric resolution on a cellulose-based stationary phase different from microcrystalline cellulose triacetate.

There are a large number of CSPs prepared by adsorption of cellulose derivatives on a macroporous silica support [17]. As CSPs, these phases are characterized by high loading capacities and fast mass transfers, *i.e.*, good efficiencies [18], and are considered as good choices for preparative applications [19]. On the other hand, the choice of solvents which can be used as mobile phase is narrowly limited [20]. In this work, we modeled the separation of the enantiomers of methyl mandelate, using 4-methylcellulose tribenzoate coated on silica as a CSP [21]. We determined the single-component adsorption isotherms of both enantiomers and their competitive isotherms. We used the equilibrium-dispersive model of chromatography [22] to calculate the response of the column to injections of each enantiomer and their mixtures. The validation of the model comes from the successful matching between experimental and calculated individual band profiles.

THEORY

The prediction of individual elution band profiles in chromatography requires first the experimental determination of the primary data of thermodynamic and kinetic nature, and second the use of a suitable numerical method for the integration of a system of partial differential equations derived from the mass balance equations of the components involved.

Calculation of band profiles

In this work, we used the equilibrium-dispersive model of chromatography [22]. This model assumes constant and instantaneous equilibrium between mobile and Stationary phases. The contributions to band broadening due to axial dispersion and to the finite rate of the mass transfer kinetics are accounted for by a lumped apparent dispersion coefficient, D_{ap}. The mass balance equation for one component, in an infinitesimal column slice, can be written as

$$\frac{\partial C}{\partial t} + \frac{1-\varepsilon_T}{\varepsilon_T} \cdot \frac{\partial q}{\partial t} + u_0 \cdot \frac{\partial C}{\partial x} = D_{ap} \cdot \frac{\partial^2 C}{\partial x^2} \quad (1)$$

where C is the concentration in the mobile phase, q is the amount adsorbed at the surface of the solid phase in equilibrium with C, u_0 is the mobile phase flow velocity and ε_T is the total porosity of the bed, taking into account the void between the beads and the intraparticle porosity; ε_T is derived from the retention time t_0 of a non-retained component whose propagation velocity is u_0. In this model, q is related to C by the equilibrium isotherm.

We also assume that D_{ap} is constant, and equal to its value under linear conditions. D_{ap} is related to the column length, L, and to the number of theoretical plates, N, by the equation

$$D_{ap} = \frac{u_0 L}{2N} \quad (2)$$

This simplification is acceptable because, at high concentrations, the thermodynamic effects, *i.e.*, the non-linear behavior of the equilibrium isotherm, influences the band profile much more strongly than the kinetic effects. Under the experimental conditions prevailing in preparative chromatography, the latter effects appear to be a correction to the band profile predicted by the equilibrium (ideal) model, and hence are properly accounted for by a lumped kinetic coefficient.

For a multi-component system, we write as many eqns. 1 as there are components. In this case, however, the different components of the mixture compete for access to the adsorption sites on the stationary phase. Thus, the amount of component i adsorbed at equilibrium depends not only on C_i, but also on the concentrations of all the other components in the mobile phase, through a competitive adsorption isotherm:

$$q_i = q_i (C_1, C_2, \ldots) \quad (3)$$

Finally, we need initial and boundary conditions to solve the problem. In elution chromatography, the column is initially empty:

$$C_i(x, t = 0) = 0 \quad (4)$$

The boundary conditions express the continuity of the flux at the column inlet and outlet. At the column inlet, the boundary condition corresponds to the injection of a rectangular pulse of the feed solution, of composition C_{F_i} and width t_F. As the column efficiency is high in HPLC, the boundary conditions can be simplified by neglecting the dispersion effect. These conditions are reduced to

$$C_i (x = 0, t) = C_{F_i} \quad 0 \leqslant t \leqslant t_F \quad (5)$$

$$C_i (x = 0, t) = 0 \quad t < 0, \quad t > t_F \quad (6)$$

Only numerical solutions are available for the equilibrium-dispersive model. The algorithms proposed have recently been reviewed [22]. For most practical applications, the finite difference method proposed by Rouchon *et al.* [23] is the fastest and most efficient algorithm, but its accuracy can be lacking in some instances, when the concentration of the second component relative to that of the first is low [24]. In this method, the dispersion term is accounted for by the numerical dispersion, through the proper choice of the size of the integration grid in the time and space domains. This numerical scheme is rigorous for a single-component system in linear chromatography [24]. In other instances, errors occur but they remain small, especially for systems such as ours, when the column has a very high efficiency (4000 theoretical plates for the most retained compound at 0.8 ml/min).

Excellent results, in agreement with experimental data, were reported previously when using the equilibrium-dispersive model and the calculation method just described for the modeling of several separations performed by liquid chromatography [12–16,24–26].

Equilibrium isotherm

The proper representation of the competitive isotherms is the keystone of our modeling effort. Our purpose is to determine the competitive isotherms which relate the compositions of the liquid and adsorbed phases at equilibrium for enantiomer mixtures. In practice, the easiest approach by far is the direct estimation of the competitive isotherms from the individual isotherms of the pure components.

Several models and equations are available to fit experimental isotherm data for single components. The classical model used in non-linear chromatography is the Langmuir adsorption isotherm [27]:

$$q = \frac{aC}{1 + bC} \quad (7)$$

where a and b are numerical coefficients. Even though this model, which assumes ideal behavior for both the solution and the adsorbed phase, is an approximation in the best of cases, it has been used successfully in many instances [25,28].

This model does not apply to our data, however (see below). An alternative which was successful for modeling the adsorption data of pure enantiomers is the bi-Langmuir model [29–31]

$$q = \frac{aC}{1 + bC} + \frac{AC}{1 + BC} \quad (8)$$

which can be considered as the extension of the Langmuir model to the case of a surface covered with patches of two different kinds.

In a second step, we need to model the competitive adsorption of binary mixtures. The competitive Langmuir isotherm model [32] is the competitive extension of the single-component Langmuir isotherms. Its parameters are those of the single-component isotherm. For a bi-Langmuir isotherm, the competitive Langmuir model can be applied separately to the two terms, assuming non-cooperative adsorption on the two types of sites [14,15,30]. The competitive isotherm is then

$$q_i = \frac{a_i C_i}{1 + b_1 C_1 + b_2 C_2} + \frac{A_i C_i}{1 + B_1 C_1 + B_2 C_2} \quad (9)$$

The Langmuir competitive isotherm model satisfies the Gibbs adsorption equation and, consequently, is thermodynamically consistent only if the column saturation capacities $qs_i = a_i/b_i$ of the two components are equal [33]. To correct for this discrepancy when they are not, Levan and Vermeulen [34] developed a binary isotherm, based on the IAS theory [35], which is valid for mixtures of gases and vapors whose individual isotherms are of the Langmuir or Freundlich types. This isotherm is written as a Taylor series. Its straightforward extension to solutions has been used previously [36]. For binary mixtures of components which have individual isotherms following the Langmuir model, the two-term expansion of the Levan-Vermeulen isotherm can be written as

$$q_1 = \frac{q_s b_1 C_1}{1 + b_1 C_1 + b_2 C_2} + \Delta_{12} \quad (10)$$

$$q_2 = \frac{q_s b_2 C_2}{1 + b_1 C_1 + b_2 C_2} - \Delta_{12} \quad (11)$$

with

$$q_s = \frac{a_1 C_1 + a_2 C_2}{b_1 C_1 + b_2 C_2} \quad (12)$$

$$\Delta_{12} = (q_{s_1} - q_{s_2}) \frac{b_1 b_2 C_1 C_2}{(b_1 C_1 + b_2 C_2)^2} \ln (1 + b_1 C_1 + b_2 C_2) \quad (13)$$

Although it may look complex, this isotherm is explicit and requires only the parameters of the single-component isotherms.

EXPERIMENTAL

Equipment

The chromatographic experiments were performed with an HP1090 liquid chromatograph (Hewlett-Packard, Palo Alto, CA, USA), equipped with a multi-solvent delivery system, an automatic sample injector with a 250-μl loop, a diode-array UV detector and a computer data acquisition system. Acquired data were downloaded to one of the VAX computers at the University of Tennessee Computer Center. Also, a Gilson (Middleton, WI, USA) Model 203 fraction collector was used to complement the HP system.

Materials

Column. A 25 cm x 0.46 cm I.D. Chiralcel OJ column (Daicel, Tokyo, Japan) was used (average particle size 10 μm). The total column porosity (ε_T = 0.70) was determind by injecting 1,3,5-tri-*tert.*-butylbenzene, a substance which can be considered to be non-retained on this stationary phase. This value of the porosity was in a very good agreement with that derived from the retention of the solvent peak.

Mobile phase and chemicals. For all chromatographic experiments, the mobile phase was hexane–2-propanol (90:10, v/v). Hexane and 2-propanol were purchased from Burdick and Jackson (Muskegon, MI, USA). L-Methyl mandelate and D-methyl mandelate (both of purity >99%), the racemic mixture (purity >98%) and 1,3,5-tri-*tert.*-butylbenzene were purchased from Fluka (Ronkonkoma, NY, USA). All compounds were used as received.

Procedures

All the experiments reported were performed at 30°C.

Determination of equilibrium isotherm data. Different chromatographic methods are available to measure the adsorption data for a pure compound [37]. In the present instance, the column efficiency was high enough to use ECP (elution by characteristic point) with good accuracy. The isotherm is derived from the diffuse rear boundary of the profile obtained when injecting a large-volume plug of a high-concentration solution,

Assuming that the rear diffuse boundary is very close to that which would be obtained for an infinitely efficient column, we can derive the concentration of the solute adsorbed on the solid phase, q, in equilibrium with the concentration, C, in the mobile phase from the retention volume of the latter through the classical equation [37]

$$q = \int_0^c \frac{V_R - V_0}{V_S} \cdot dC \quad (14)$$

where V_R, V_0 and V_S are the retention volume, the column hold-up volume and the solid-phase volume, respectively.

The equilibrium data were determined at a flow-rate of 0.8 ml/min. The average width of the injected plug was *ca.* 5 min and its concentration was *ca.*

4 g/l. Because the HP1090 system is not equipped with a large enough sample loop, the injections were made by programming the multi-solvent delivery system. The diode-array detector signal was recorded with a 640-ms period, at a wavelength of 270 nm. The response signal was converted into concentrations through a calibration graph. The slightly non-linear detector response was fitted to a third-order polynomial. Following conversion into concentration units, the equilibrium data were calculated individually for each enantiomer. About 50 experimental points, evenly spaced over the concentration range, were used to determine the equilibrium isotherm.

Competitive adsorption data were measured using a binary frontal analysis method [38]. In all experiments, the initial concentration of the enantiomers in the column was zero. Thus, the concentration of the more retained component in the intermediate plateau [38] was also zero and there was no need to analyze the corresponding eluate. The concentration of the less retained component in this intermediate plateau was derived from the calibration graph at 250 nm, at which wavelength the detector response was linear over the whole concentration range studied. The retention volumes and the corresponding concentrations were inserted into the equation given by Jacobson et *al.* [38] to determine the amount adsorbed. The measurements of adsorbed amounts could not be made for values of the total concentration higher than *ca.* 1.2 g/l. At higher concentrations, the intermediate plateau [38] disappeared.

Determination of elution profiles. The elution profiles of the pure enantiomers were obtained by injecting increasingly large volumes of a given solution. The detector signal was converted into a concentration profile through the calibration graph, linear over the concentration range used. This graph is the same for both enantiomers. Mixtures prepared by mixing the two pure enantiomers in 1:3 and 4:1 ratios were also injected. All injections were performed at a flow-rate of 0.8 ml/min, corresponding to an approximate value of 8 for the Peclet number (d_p = 10 μm, $D_m = 1 \cdot 10^{-5}$ cm^2/s).

For mixtures, the individual elution profiles were determined in the mixed-band region by collecting fractions of the eluent and reinjecting them onto the same column, but under analytical conditions. Fractions were collected at 9-s intervals, from the start of the elution of the first component through the estimated end of the mixed zone. The relative concentration of the two enantiomers in a fraction is equal to the peak-area ratio. Combined with the recorded total signal of the detector, this allows the determination of the individual concentration profiles.

RESULTS AND DISCUSSION

Modeling of single-component equilibrium isotherms

The Scatchard plot of the single-component data (Fig. 1) is not linear, which shows that the classical Langmuir model cannot account for the isotherms. A two-site adsorption model, including enantioselective and non-selective sites, appears to be plausible in the present instance. This justifies the use of a bi-Langmuir isotherm, a model already used successfully for the modeling of other enantiomeric separations [12,13].

For all compounds, there are a variety of molecular interactions with a stationary phase, the combination of which accounts for the retention. Both enantiomers have complex interactions with the chiral stationary phase (CSP), some of which are

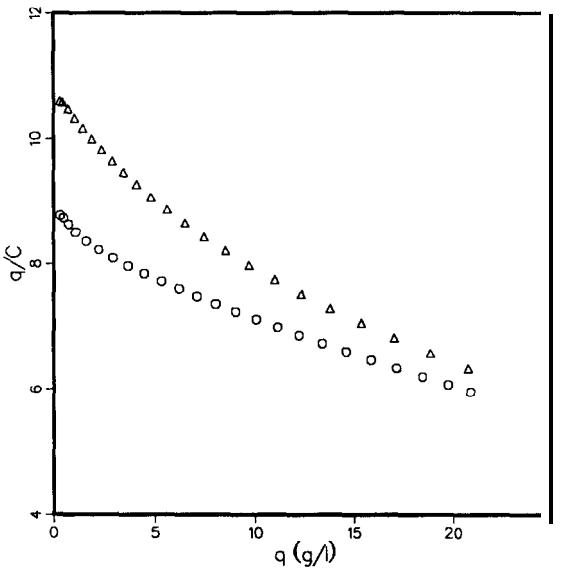

Fig. 1. Scatchard plots (i.e., ***q/C versus q)*** of the experimental adsorption data for (0) (−)-methyl-D-mandelate [(-)-MM] and (△) (+)-methyl-L-mandelate [(+)-MM].

achiral (hence identical for both enantiomers), while others involve the stereochemistry of the enantiomers and the CSP, causing the formation of a transient diastereomeric solute-CSP complex. If the stability of the complex is different for the two enantiomers, they will be separated. For the more strongly retained enantiomer, at least, the formation energy of this complex is higher than the energy of conventional intermolecular interactions [5,19,20]. Thus, a bi-Langmuir isotherm is likely; the first term would represent the retention linked with the chiral recognition mechanism, while the second term would include all the non-enantioselective interactions. Previous investigations of the chiral recognition process on cellulose-band CSP have disclosed the existence of two types of retention mechanisms [39,40].

If this assumption is correct, no chiral selectivity should be involved in the second term of a bi-Langmuir isotherm model. The coefficients A and *B* (eqns. 8 and 9) should be the same for both enantiomers, in which event the total number of parameters of the model is reduced to 6. Thus, we fitted together the two sets of experimental data, one for each enantiomer. We used a program based on a simplex algorithm to minimize the following objective function:

$$\delta = \delta_D + \delta_L = \sqrt{\frac{1}{N_D}\sum_{1}^{N_D}\left(\frac{q_{exp_i} - q_{cal_i}}{q_{exp_i}}\right)_D^2} + \sqrt{\frac{1}{N_L}\sum_{1}^{N_L}\left(\frac{q_{exp_i} - q_{cal_i}}{q_{exp_j}}\right)_L^2} \quad (15)$$

where the subscripts D and L refer to the (−)-methyl-D-mandelate and the (+)-methyl-L-mandelate, respectively, while N_D and N_L are the numbers of data points for the D- and L-enantiomers, respectively. The use of a weighted function (eqn. 15) permits a good accuracy of the fit at both low and high concentrations. The use of an alternate objective function, $\delta_D + \delta_L + |\delta_D - \delta_L|$, was abandoned because local optima appeared.

The values derived for the isotherm parameters are summarized in Table I. The experimental (symbols) and calculated (dotted lines) isotherm data are compared in Fig. 2. They are in excellent agreement. The (+)-enantiomer is the more retained on this stationary phase. It can be seen in Table I that, as reported previously [12], the adsorption energy on the non-enantioselective sites is lower than that on the enantioselective sites (i.e., *B* is lower than b), but that the saturation capacity of these non-selective sites is much higher.

Modeling of competitive equilibrium isotherm

The competitive isotherm contains two terms, one for the enantioselective and the other for the non-selective sites. The latter term is obviously the Langmuir term corresponding to the sum of the concentrations of the two enantiomers.

The extrapolated values of the saturation capacity for the enantioselective sites are not the same for the two enantiomers (Table I). Therefore, we cannot use for them a competitive Langmuir isotherm which would not be thermodynamically consistent

TABLE I

ISOTHERM PARAMETERS

Model of competitive isotherm:

$$q_{(x)} = LV_{(x)}[C_{(-)}, C_{(+)}] + \frac{Q_s B C_{(x)}}{1 + B[C_{(-)} + C_{(+)}]}$$

where $x = -, +$; LV refers to the Levan-Vermeulen isotherm calculated with the coefficients of the individual isotherms on the selective sites.

Number of parameters	Type of sites	Isomer	a	*b* (l/g)	q_s (g/l)
6 (Model 1)	Selective	(-)-	1.83	0.786	2.33
	Selective	(+)-	3.86	1.11	3.48
	Non-selective	(−)- and (+)-	6.91	0.076	91.2

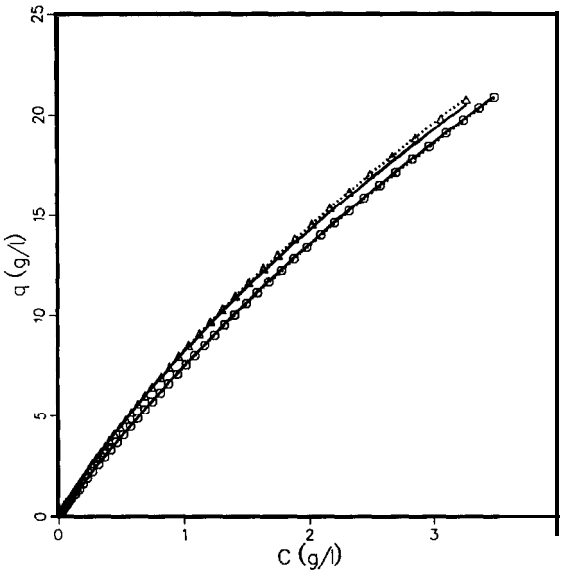

Fig. 2. Experimental adsorption data for (0) (-)-MM and (△) (+)-MM on a Chiralcel OJ phase at 30°C. The lines correspond to the isotherm equations derived from Models 1 (dotted lines) and 2 (solid lines).

[34,35]. In such a case, the Levan-Vermeulen isotherm [34] is the simplest competitive isotherm model that can be used and we adopted it for the enantioselective sites (Table I).

However, the adsorption data were measured in a range of concentrations which, although high enough to encompass the range covered by chromatographic bands at the time of their elution, was limited to *ca.* 3.5 g/l. The amount adsorbed at this concentration corresponds to only 20% of the estimated saturation capacity, which, accordingly, was determined by extrapolation. Such values are inaccurate and must be considered with caution. Further, although large in relative terms (30%), the difference between the extrapolated values of the saturation capacities of the enantioselective sites for the two enantiomers is small compared with the total saturation capacities, which increases the inaccuracy of the estimate.

Not knowing the nature of the chiral retention mechanism, we used a second approach, previously developed in the study of the separation of racemic mixtures of amino acids on immobilized BSA [12,13]. We assumed that the saturation capacities of the two enantiomers were equal for the enantioselective sites, $a_{(-)}/b_{(-)} = a_{(+)}/b_{(+)}$, and we fitted our data to a five-parameter isotherm model (Table II). We could not derive these parameters in a straightforward way, however. Actually, when we fitted our data with a five-parameter model, we obtained parameter values different from the previous values (in Table I), including a saturation capacity for the non-enantioselective sites which was twice as large as that obtained in the first approach. These parameters did not provide a satisfactory calculation of the elution profiles. This result can be understood if we consider that the objective function being the same for both models, the optimization procedure for the five-parameter model is limited to the sub-domain of the six-parameter space where we have the relation $qs_{(-)} = qs_{(+)}$. Hence, the optimum

TABLE II

ISOTHERM PARAMETERS

Model of competitive isotherm:

$$q_{(x)} = \frac{q_s B_{(x)} C_{(x)}}{1 + b_{(-)}C_{(-)} + b_{(+)}C_{(+)}} + \frac{Q_s B C_{(x)}}{1 + B[C_{(-)} + C_{(+)}]}$$

wherex = −, +.

Number of parameters	Type of sites	Isomer	a	b (l/g)	q_s (g/l)
5 (Model 2)	Selective	(-)-	2.14	0.506	4.22
	Selective	(+)-	4.31	1.022	4.22
	Non-Selective	(−)- and (+)-	6.50	0.071	91.2

of the objective function in this sub-domain can be far from the real optimum.

Because of its flexibility, we can expect the six-parameter model to give a relatively good approximation of the saturation capacity on the non-stereoselective sites. Then, in order to obtain more realistic values of the isotherm parameters, we assumed the value of this saturation capacity to be correct, and determined the remaining four parameters of the five-parameter model (Table II). Indeed, the two models give almost identical individual isotherms (Fig. 2, second isotherm in solid lines), except for a slight difference in the high concentration range, for the (+)-enantiomer. As the saturation capacities are now equal, however, we can derive a competitive bi-Langmuir isotherm from the second model.

These two models, referred to below as Models 1 (Table I) and 2 (Table II), were used to predict the competitive isotherms. In Fig. 3, we compare the experimental data on competitive adsorption obtained by binary frontal analysis (symbols) and the isotherms calculated with the two models (solid lines). The comparison is made for different values of the relative composition of the mobile phase. The two models gave identical results, which are also in very good agreement with experimental data. In most instances, the difference was less than 2%. The structures of the two competitive isotherm models are different, and they give different amounts adsorbed on the two types of sites for a given concentration. However, because of a fortuitous compensation, the two models give virtually identical values for the total amount adsorbed, in the concentration range investigated. A significant difference would arise only at concentrations much higher than those at which accurate measurements could be carried out.

Single-component band profiles

Fig. 4 shows a chromatogram obtained under linear conditions, with a very small amount injected (2 μg). The retention times derived from it are in excellent agreement with the initial slopes of the enantiomer isotherms. The selectivity is low (α = 1.22), but the efficiency is high for both components and the resolution complete (R_s = 2.5). The plate numbers determined with the conventional method are $N_{(-)}$ = 4500 and $N_{(+)}$ = 4000 at a velocity of 0.08 cm/s (F_v = 0.8 ml/min), giving reduced plate heights of 5.6 and 6.2, respectively, for a Peclet number close to 8.

As the single-component isotherm data were de-

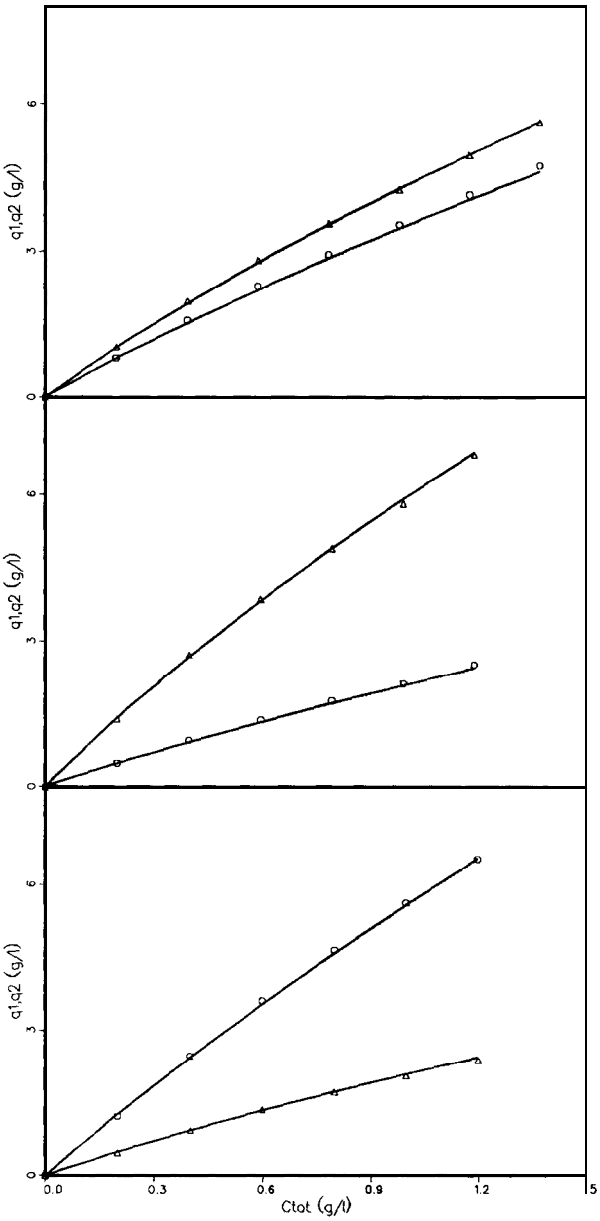

Fig. 3. Experimental competitive adsorption data (○)(−)-MM and (A) (+)-MM and calculated isotherms (dotted lines for Model 1, solid lines for Model 2), for different mixtures of constant compositions. Ratios C(+)/C(-): top = 1.05; middle = 2.43; bottom = 0.32.

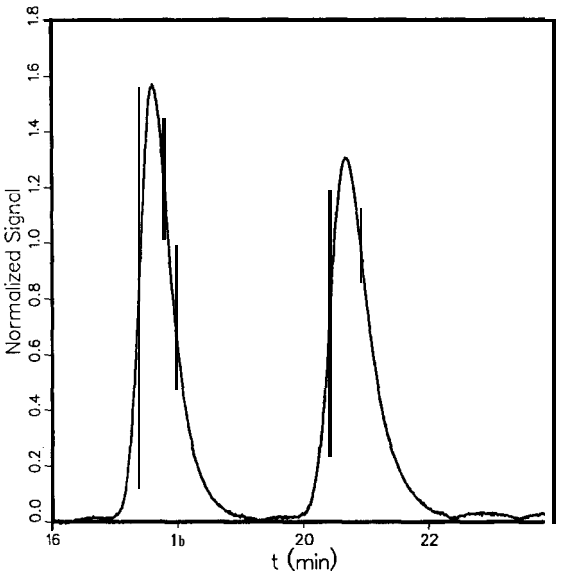

Fig. 4. Normalized chromatogram under linear conditions for the racemic mixture. Volume injected, 50 μl; total concentration, 40 mg/l; total amount, 2 μg.

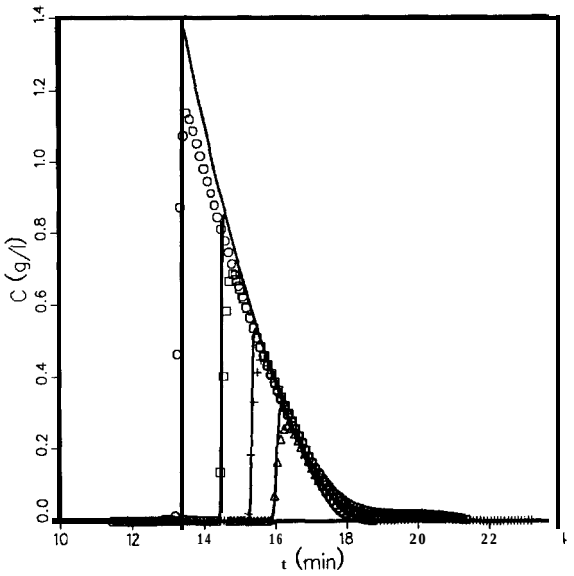

Fig. 5. Experimental (symbols) and calculated (solid lines) elution profiles for injections of samples of different volumes of a 2.6 g/l (-)-MM solution. Model 2 (Table II) was used for the calculations. Volumes injected: 100, 200, 400 and 800 μl.

rived by ECP, a method based on the ideal model, comparing recorded band profiles obtained on injection of large-sized samples with the results of calculations based on the equilibrium-dispersive model, is a circular argument. We can, however, compare the band profiles calculated from the isotherm data with the profiles recorded 2 months later, using the same column but another instrument, in a different location. This illustrates the kind of reproducibility achieved for chromatographic data and the modeling accuracy that can be expected in attempts at designing separation units.

Figs. 5 and 6 compare recorded (symbols) and calculated (lines) chromatograms for four consecutive injections of increasing volumes of given solutions (ca. 2.5 g/l) of the pure (−)- and (+)-enantiomers, respectively. In order to achieve overlay of the diffuse boundaries of the four profiles, the time scale is corrected of the width of the injected plug. The elution profiles were calculated with the second isotherm model. They agree well with the experimental data and confirm the validity of the individual isotherms measured. They also show the good stability of the cellulose column, if used under

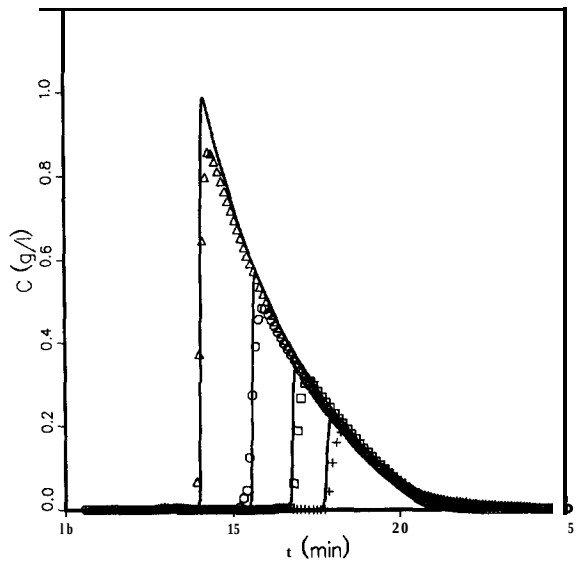

Fig. 6. Experimental (symbols) and calculated (solid lines) elution profiles for injections of samples of different volumes of a 2.6 g/l (+)-MM solution. Model 2 was used for the calculations. Volumes injected: 100, 200, 400 and 800 μl.

regular and smooth conditions. The baseline bump behind the (-)-enantiomer profile in Fig. 5 is due to a small amount of (+)-isomer (1.5%). The individual band profiles of the two enantiomers calculated with the two isotherm models are compared in Fig. 7. These results reflect the agreement observed between the single-component isotherms (Fig. 2): the profiles differ by the thickness of the line in the case of the less retained enantiomer, and hardly more for the other enantiomer.

Individual band profiles in binary mixtures

There are two important separation problems for enantiomers, the separation of the racemic mixture and the purification of one enantiomer from moderate or low concentrations of the other. Our purpose was to model either type of separation for large sample sizes, *i.e.*, under overloaded conditions. Separations of the racemic mixture are presented in the Figs. 8 and 9. Figs. 8 and 9 show the chromatograms (symbols) obtained for increasingly large amounts of the racemic mixture, going from nearly "touching band" separation [41] to an important degree of band overlapping. The lines show the profiles calculated using the competitive isotherm derived from Model 2.

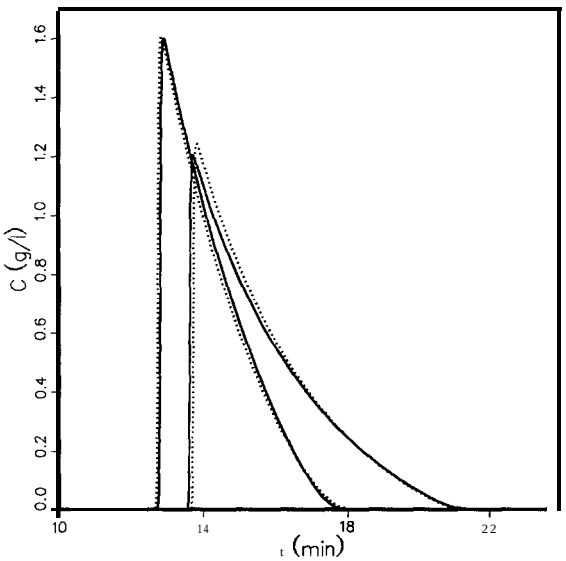

Fig. 7. Comparison of the individual elution profiles calculated with the isotherms derived from Models 1 (dotted lines) and 2 (solid lines) for the two enantiomers [(-)-MM is the less retained]. Concentration of injected solution, 2.50 g/l; volume injected. 1.0 ml.

There is general agreement between the experimental and simulated profiles, although a systematic deviation is observed for the chromatograms in Fig. 8, as the less retained (−)-enantiomer elutes too early. This anomaly does not appear in Fig. 9. The difference between calculated and experimental chromatograms is a mere retention time shift of *ca.* 1.5%. It can be simply explained by the difficulty encountered in resetting exactly the flow-rate and the dead volumes. For the two largest amounts in Fig. 8, and to a lesser extent in Fig. 9, the shapes of the experimental and calculated rear diffuse boundaries are also different in the high concentration range.

We see that the inflection point is slightly higher on the calculated profiles than on the experimental ones. The inflection point on this rear boundary corresponds to the intermediate plateau of the more retained component predicted by the ideal model but which cannot be observed for this mixture composition, because the column efficiency is too low. The concentration of this plateau, and hence of the inflection point, depend only on the competitive equilibrium isotherm. The divergence observed is due to a small error in the competitive isotherm.

To check further the validity of band profiles calculations, we determined experimentally, by analysis of collected fractions, the individual band profiles of the two enantiomers for 2-mg samples of three different binary mixtures, having relative compositions 1:1 (Fig. 10), 4:1 (Fig. 11) and 1:3 (Fig. 12). The total injection concentration was 8 g/l and the maximum concentration of the eluted bands was of the order of 1 g/l, which corresponds to a high degree of column overload. The injection concentration exceeds the range within which were determined single-component (O-3.5 g/l, Fig. 1) and competitive isotherms (O-l.2 g/l, Fig. 3). Dilution occurs quickly, however, and during most of the band migration its concentration is within the range studied.

In Figs. 10–12, we compare the experimental profiles with those calculated with Models 1 (dotted lines) and 2 (solid lines). The two models give slightly different calculated profiles, which suggests that the two isotherm models are less similar than observed in Fig. 3 at high concentrations. The general

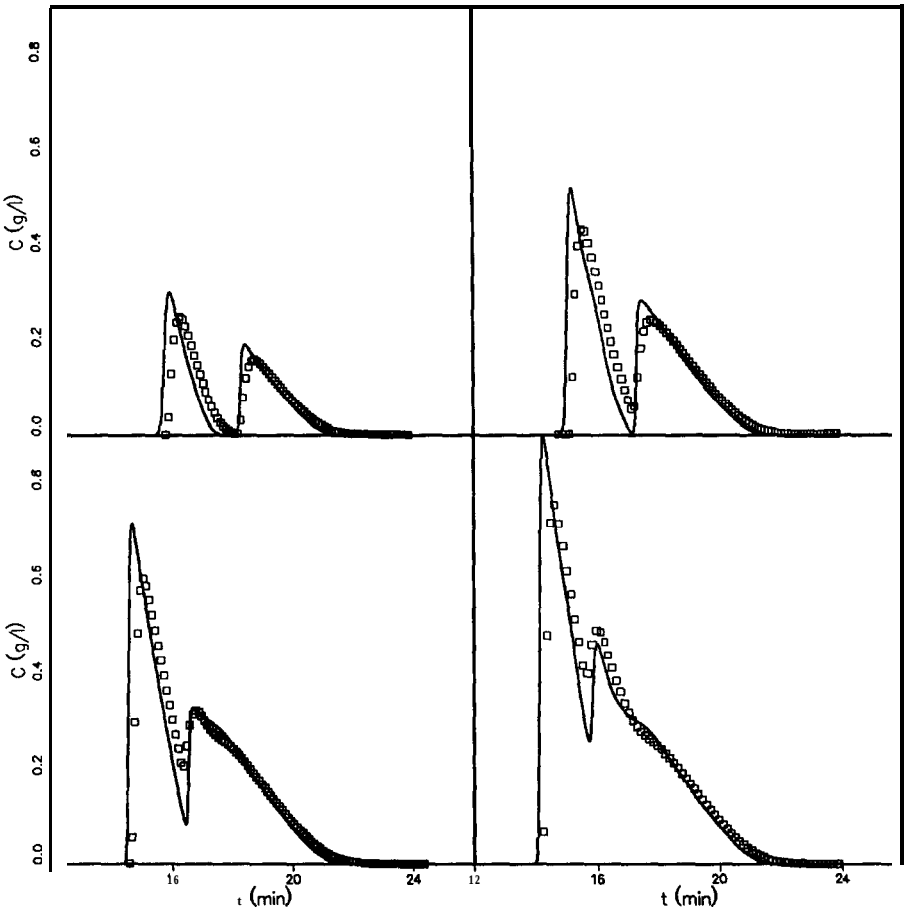

Fig. 8. Experimental (symbols) and calculated (lines) chromatograms (total concentration of the two enantiomers) for different volumes injected of a racemic mixture of methyl (−)- and (+)-mandelate. $C(-) = C(+) = 4.1$ g/l. Volumes injected: 50, 100, 150 and 200 μl. The solid lines were calculated using the competitive isotherm Model 2 (Table II).

agreement is better with the profile calculated with Model 2 than Model 1. Both models give an excellent prediction of the individual profiles for the 4: 1 mixture (Fig. 11), possibly because the concentration of the second component is much lower in this instance than in the other two (Figs. 10 and 12). On the other hand, the agreement between calculated and experimental profiles for the 1:3 mixture (Fig. 12), for which the second component concentration is much higher, is less satisfactory.

Differences are noted at the end of the rear diffuse boundary of the (+)-enantiomer, whereas excellent agreement was observed in Figs. 10 and 11. Indeed, this part of the band profile depends only on the isotherm of the more retained solute. Fig. 9 shows the global signal observed for the experiment reported in Fig. 10. In Fig. 10, we see clearly that the inflection point on the diffuse boundary of the (+)-enantiomer is higher for the calculated than for the recorded profile, regardless of the model chosen for calculations. This points to an error in the competitive isotherms, causing in turn an error in the concentrations of the two components in the mixed zone of the chromatogram: we observe in Figs. 10 and 12 that the calculated concentrations of the (-)-enantiomer in the mixed zone between the bands of pure enantiomers are too low whereas those of the (+)-enantiomer are too high. This

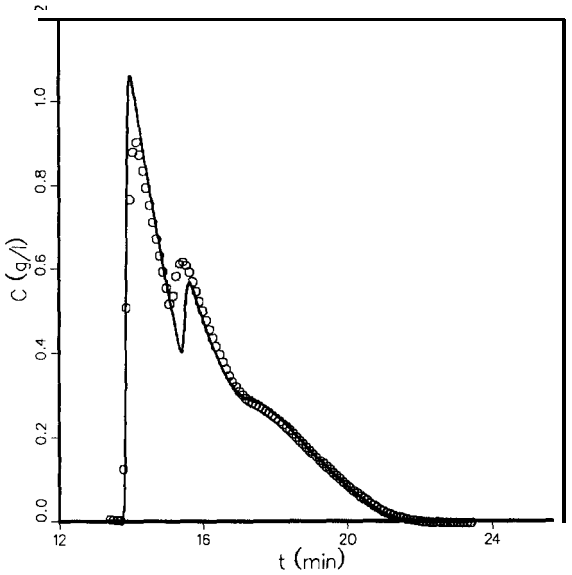

Fig. 9. Same as Fig. 8, but C(-) = 4.2 g/l and C(+) = 3.8 g/l: volume injected, 250 μl.

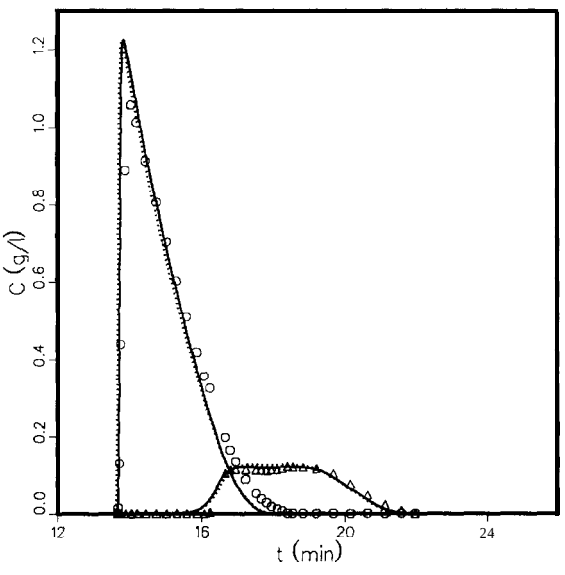

Fig. 11. Same as Fig. 10, but C(−) = 6.2 g/l and C(+) = 1.5 g/l.

means that our competitive isotherm induces too much displacement effect. This is especially true for Model 1.

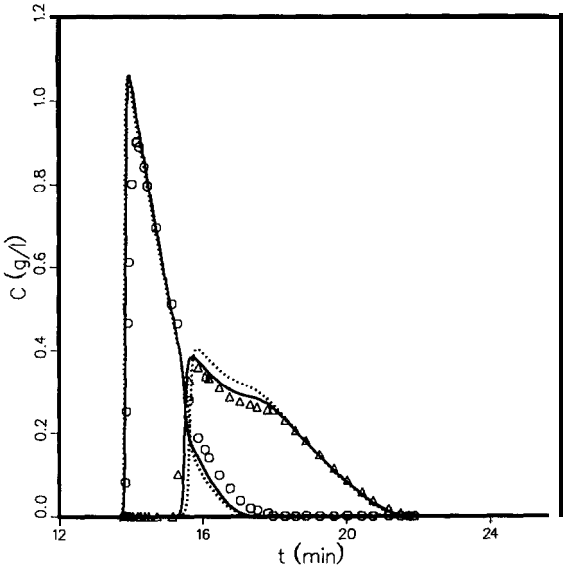

Fig. 10. Comparison between experimental [○ = (-)-MM; △ = (+)-MM] and calculated (dotted lines for Model 1, solid lines for Model 2) individual elution profiles for an injection of a binary mixture. Sample composition, C(-) = 4.2 g/l and $C(+)$ = 3.8 g/l; sample **volume,** 250 μl.

In Fig. 3, the agreement between predicted and experimental data for the adsorption of mixtures is very good, and we expected a still better agreement between experimental and calculated profiles than observed in Figs. 8-12, even though experimental parameters other than the isotherms are involved.

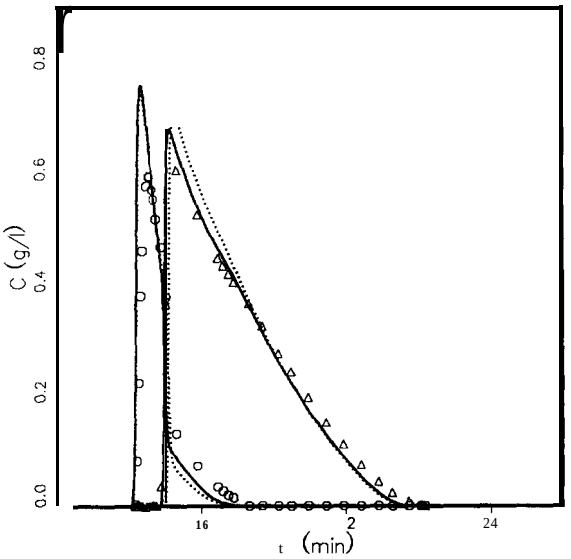

Fig. 12. Same as Fig. 10, but $C(-)$ = 1.8 g/l and C(+) = 5.9 g/l.

TABLE III

ISOTHERM PARAMETERS

Model of competitive isotherm:

$$q_{(x)} = \frac{q_s B_{(x)} C_{(x)}}{1 + b_{(-)}C_{(-)} + b_{(+)}C_{(+)}} + \frac{Q_s B C_{(x)}}{1 + B[C_{(-)} + C_{(+)}]}$$

wherex = −, +.

Number of parameters	Type of sites	Isomer	a	b (l/g)	q_s (g/l)
5	Selective	(-)-	2.05	0.741	2.76
	Selective	(+)-	3.90	1.414	2.76
	Non-Selective	(-)-and (+)-	7.12	0.079	89.9

For these experiments, we used small volumes of highly concentrated samples. To confirm the validity of our competitive isotherms in the concentration range where binary adsorption data could be determined more accurately (Fig. 3), we injected a large volume of a dilute sample of the racemic mixture (Fig. 13). The amount injected is almost the same as for Fig. 10, but the concentration is about seven times lower.

To check the degree of stability of the column

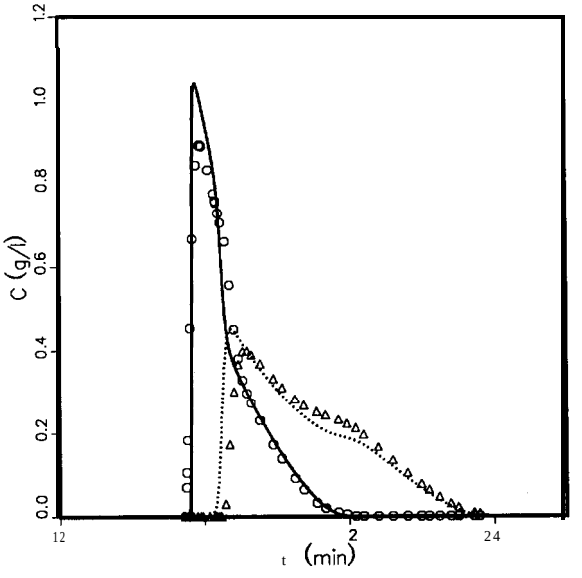

Fig. 13. Comparison between experimental [0 = (-)-MM; △ = (+)-MM] and calculated (Table III) individual profiles for an injection of a binary mixture. Sample composition, C(−) = 0.66 g/l and C(+) = 0.68 g/l; sample volume, 1.60 ml.

performance during the few months that elapsed between the two experiments, we measured again the adsorption equilibrium data for each enantiomer at the time of the second experiment, for concentrations up to 1.3 g/l. The new values of the parameters were calculated for the isotherm, following the procedure described above for Model 2 (see Table III). These values are very close to the former values (Table II) but not close enough to avoid the use of the old parameter values resulting in significant differences in the calculated elution profiles. With the new parameter values, the agreement observed in Fig. 13 is only slightly better than that in Fig. 10.

All these results prove that the competitive isotherm model chosen (Model 2) gives a very good approximation of the adsorption behavior of the enantiomers, and permits a calculation of adsorption data for mixtures that is precise enough for the modeling of preparative chromatography.

CONCLUSIONS

As previously reported in a number of instances [41], there is generally very good agreement between experimental and calculated individual band profiles for large-sized injections of binary mixtures in the whole range of relative compositions. The extent of this agreement is limited by the accuracy of the modeling of the competitive isotherms. This has several important consequences, as follows.

The accuracy of the equilibrium-dispersive model is more than adequate. At least for low relative

molecular mass compounds, there is no need for a more exact kinetic model. This simplifies considerably the collection of the data required for modeling, as only the plot of the column height equivalent to a theoretical plate *versus* the flow velocity is needed.

The modeling of the competitive isotherm is critical. Unless a simple, clearly identifiable, selective retention mechanism is used, simple models may lack accuracy, and it may be impossible to predict the competitive adsorption behavior merely from the single-component isotherms.

At this stage, accurate experimental data are needed, as reliable isotherm models are lacking. These data must encompass the entire range of concentrations experienced in a band during its migration, *i.e.*, must go from zero to the injection concentration.

Although imperfect, current models permit the calculation of band profiles which are in sufficient agreement with experimental data to warrant their use in optimization procedures.

The difficulty in selecting an adsorption isotherm model that is accurate for enantiomeric separations on cellulose is related to our present ignorance regarding the origin of its enantioselectivity. With five carbon atoms out of six exhibiting chirality, cellulose provides a highly chiral environment, and it is difficult at this stage to suggest any particular mechanism to explain its enantioselectivity. In the light of that lack of understanding, it is most interesting to observe that there seems to be no enantioselective component in the low-energy molecular interaction term, while the high-energy interaction term accounts for all the enantioselectivity. Whether there are also some high-energy, non-selective molecular interactions involved remains an unanswered question. We note, however, that the enantioselective retention mechanism, although described by the same empirical isotherm as for mandelic acid on immobilized BSA, is profoundly different. With BSA, the enantioselective retention mechanism involves strong interactions between the enantiomers and a hydrophobic pouch in the protein molecule [42], thus validating the basic assumptions of the Langmuir model for the enantioselective sites [43]. Also noteworthy is the considerable difference observed between the adsorption behavior of the enantiomers of methyl mandelate on Chiralcel OJ and of those of Trbger's base on microcrystalline cellulose triacetate [8].

ACKNOWLEDGEMENTS

This work was supported in part by Grant CHE-9201663 of the National Science Foundation and by the cooperative agreement between the University of Tennessee and the Oak Ridge National Laboratory. F.C. thanks Rhône-Poulenc for financial support of this work. We are grateful to Hewlett-Packard for the gift of a Model 1090A liquid chromatograph with its data system and to ADA for the software that permits the transfer of the data files recorded by the liquid chromatograph to the computer center. We acknowledge continuous support of our computational efforts by the University of Tennessee Computing Center.

REFERENCES

1 M. Simonyi, ***Med. Res. Rev., 4 (1984) 359.***
2 E. J. Ariens, ***Med. Res. Rev., 6 (1986) 451.***
3 W. H. De Camp, ***Chirality***, 1 (1989) 2.
4 M. Lienne, M. Caude, A. Tambute and R. Rosset, ***Analusis***, 15 (1987) 431.
5 I. W. Wainer and C. Alembik, in M. Zief and L. J. Crane (Editors), ***Chromatographic Chiral Separations,*** Marcel Dekker, New York, 1988, p. 355.
6 G. Vigh, G. Quintero and G. Farkas, ***ACS Symp. Ser., 434, (1990) 181.***
7 R. M. Nicoud and M. Bailly, in M. Perrut (Editor), ***Proceedings PREP'92, Nancy, France, April 1992,*** Société Française de Chimie, Paris, p. 205.
8 A. Seidel-Morgenstern and G. Guiochon, to be published.
9 S. Golshan-Shirazi and G. Guiochon, ***J. Chromatogr., 517 (1990) 229.***
10 S. Golshan-Shirazi and G. Guiochon, ***J. Chromatogr., 536 (1991) 57.***
11 A. Felinger and G. Guiochon, ***J. Chromatogr., 591 (1992) 31.***
12 S. Jacobson, A. Felinger and G. Guiochon, ***Biotech. Bioeng., 40 (1992) 1210.***
13 S. Jacobson, A. Felinger and G. Guiochon, ***Biotech. Prog.,*** in press.
14 S. Jacobson, S. Golshan-Shirazi and G. Guiochon, ***AIChE J., 37 (1991) 836.***
15 S. Jacobson, S. Golshan-Shirazi and G. Guiochon, ***J. Am. Chem. Soc.***, 112 (1990) 6493.
16 A. Seidel-Morgenstem and G. Guiochon, to be published.
17 Y. Okamoto, M. Kawashima and K. Hatada, ***J. Am.*** Chem. ***Soc.***, 106 (1984) 5357.
18 Y. Okamoto, M. Kawashima, R. Aburatani, K. Hatada, T. Nishiyama and M. Masuda, Chem. ***Left.,*** (1986) 1237.
19 E. Francotte and A. Junker-Buchheit, ***J. Chromatogr., 576 (1992) I.***

20 D. M. Johns, in W. J. Lough (Editor), ***Chiral Liquid Chromatography,*** Rutledge, Chapman & Hall, London, 1989, p. 166.
21 Y. Okamoto, R. Aburatani and K. Hatada, ***J. Chromatogr., 389 (1987) 95.***
22 S. Golshan-Shirazi and G. Guiochon, in F. Dondi and G. Guiochon (Editors), ***Theoretical Advancement in Chromatography and Related Separation Techniques, NATO ASI, No. C. 383,*** Kluwer, Delft, 1992, p. 35.
23 P. Rouchon, M. Schonauer, P. Valentin and G. Guiochon, ***Sep. Sci. Technol., 22 (1987) 1793.***
24 M. Czok and G. Guiochon, ***Comput. Chem. Eng.,*** 14 (1990) 1435.
25 A. M. Katti, M. Czok and G. Guiochon, ***J. Chromatogr., 556 (1991) 205.***
26 M. Diack and G. Guiochon, ***Anal. Chem., 63 (1988) 2634.***
27 I. Langmuir, ***J. Am.*** Chem. ***Soc.***, 38 (1916) 2221.
28 S. Golshan-Shirazi and G. Guiochon, ***Anal.*** Chem., 60 (1988), 2634.
29 D. Graham, ***J. Phys. Chem., 57 (1953) 665.***
30 J. D. Andrade, ***Surface and Interfacial Aspects of Biomedical Polymers,*** Plenum Press, New York, 1985, Ch. I.
31 R. J. Laub, ***ACS Symp. Ser., 297 (1986)*** 1.
32 G. M. Schwab, ***Ergebnisse des Exacten Naturwissenschaften,*** Vol. ***7,*** Springer, Berlin, 1928, p. 276.
33 C. Kembell, E. K. Rideal and E. A. Guggenheim, ***Trans. Faraday Soc., 44 (1984) 948.***
34 M. D. Levan and Vermeulen, ***J. Phys.*** Chem., 85 (1981) 3247.
35 A. L. Meyers and J. M. Prausnitz, ***AIChE J.,*** 11 (1965) 121.
36 S. Golshan-Shirazi, J.-X. Huang and G. Guiochon, ***Anal.*** Chem., 63 (1991) 1147.
37 A. M. Katti and G. Guiochon, ***Adv. Chromatogr., 32 (1991)*** 1.
38 J. Jacobson, J. M. Frenz and C. Horváth, ***Znd. Eng. Chem. Res., 26 (1987) 43.***
39 I. W. Wainer, R. M. Stiffin and T. Shibata, ***J. Chromatogr., 411 (1987) 139.***
40 Y. Fukui, A. Ichida, T. Shibata and K. Mori, ***J. Chromatogr., 515 (1990) 85.***
41 G. Guiochon, A. M. Katti, M. Diack, M. Z. El Fallah, S. Golshan-Shirazi, S. C. Jacobson and A. Seidel-Morgenstern, ***Acc.*** Chem. ***Res.,*** 25 (1992) 366.
42 S. Allenmark and S. Andersson, ***Chirality, 4 (1992) 24.***
43 S. C. Jacobson, S. Andersson, S. Allenmark and G. Guiochon, in preparation.